P: ISSN No. 0976-8602 RNI No. UPENG/2012/42622 VOL.-III, ISSUE-III, JULY-2014
E: ISSN No. 2349-9443
Asian Resonance

Synthesis and Antifungicidal Activity of Some Transition Metal Complexes with Benzimidazole Dithiocarbamate Ligand

Yogendra Sharma
Deptt. of Chemistry,
Meerut College
Meerut, U.P.

Sandeep Kashyap
Deptt. of Chemistry,
Meerut College
Meerut, U.P.

Meenakshi Thakur
Deptt. of Chemistry,
Meerut College
Meerut, U.P.

Rajeev Kumar
Deptt. of Chemistry,
Meerut College
Meerut, U.P.

B.P.Yadav
Deptt. of Chemistry,
Meerut College
Meerut, U.P.

Abstract

Synthesis of HL ligand and some transition metal complexes and their biological and antifungicidal activity have been studied with Benzimidazole dithiocarbamate ligand. In the present work fungicidal activity and the structures of the complexes of HL with Cr(III), Mn(II), Co(II), Ni(II), Cu(II) (Cl^- and SO_4^{2-}) and Zn(II) ions are confirmed by the elemental analyses, IR, molar conductance, magnetic, solid reflectance, mass and thermal analysis data.

Keywords: Synthesis of HL ligand, Benzimidazole dithiocarbamate, biological activities and analyses.

Introduction

Many biological active heterocyclic compounds containing the dithiocarbamate and/or benzimidazole moieties as well as their transition metal complexes were reported[1–3]. As a result, many fungicides[1,4,5] bactericides[3,5], acaricides[6], nematocides[7], insecticides[6–9] and other pharmaceutical as well as agricultural compositions were found to contain one or more of these bioactive groups[10,11]. In view of this fact, it was concerned with the synthesis of new benzimidazole derivatives containing the dithiocarbamate functional group which found to be promising as antifungal agent[12]. It was thought of interest to explore the ligational behaviour of one of these derivatives with some transition metals aiming to increase its fungicidal potency. Metal chelates with Cr(III), Mn(II), Co(II), Ni(II), Cu(II), Zn(II) transition metals are prepared and characterized using different physico–chemical techniques like elemental analyses (C, H, N, S and metal content), IR, magnetic moment and reflectance spectra and thermal analyses (TGA and DTA). Biological activities of the complexes are studied. The structure of HL ligand is given in Fig.1.

Experimental

Materials and reagents

All chemicals used were of the analytical reagent grade (AR), and of highest purity available. They included copper(II) chloride and sulpahte di– and penta–hydrates (prolabo); cobalt(II) and nickel(II) chloride hexahydrates (BDH); zinc chloride dihydrate (Unichem), manganese(II) and chromium(III) chloride (Sigma). Zinc oxide, disodium salt of ethylenediaminetetraacetic acid; EDTA; (Analar), ammonia solution (33%, v/v) and ammonium chloride. Organic solvents used included absolute ethyl alcohol, diethylether, dimethylformamide (DMF) and dimethylsulphoxide (DMSO). Hydrochloric and nitric acids (MERCK) were used. De–ionized water collected from all glass equipments was usually used in all preparations. Antifungal susceptibility testing was performed in potato–dextrose agar (PDA) media containing drops of 25% lactic acid to prevent the bacterial contamination. A series of concentrations for each investigated compounds was carried out using DMSO as a solvent.

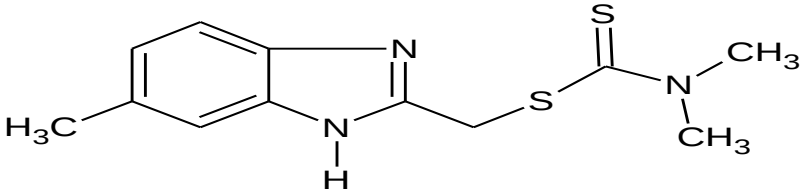

Fig. 1. Structure of HL Ligand

Instruments

The molar conductance of solid complexes in DMF was measured using Sybron–Barnstead conductometer (Meter–PM–6. E=3406). Elemental microanalyses of the separated solid chelates for C, H, N and S were performed in the Microanalytical Center, C.R.R.I. Lucknow. The analyses were repeated twice to check the accuracy of the data. Infrared spectra were recorded on Perkin–Elmer FT–IR type 1650 spectrophotometer in wave number region 4000–200 cm^{-1}. The spectra were recorded as KBr pellets. The solid reflectance spectra were measured on a Shimadzo 3101 pc spectrophotometer. The molar magnetic susceptibility was measured on powdered samples using the Faraday method. The diamagnetic corrections were made by Pascal's constant and $Hg[Co(SCN)_4]$ was used as a calibrant. The thermal analyses (TGA, DrTGA and DTA) were carried out in dynamic nitrogen atmosphere (20 mL min^{-1}) with a heating rate of 10 C min^{-1} using Shimadzu TGA–50H and DTA–50H theral analyzers.

Synthesis of HL ligand

The used ligand which is formulated as dimethyl S–(1H–4–Methylbenzi– midazol–2–yl)methyl dithiocarbamate was prepared by the standard reported[12] method (Fig.1)

Synthesis of Metal Complexes

Hot solution (60 C) of the appropriate metal chloride or sulphate (1 mmol) in an ethanol–water mixture (1:1, 25 mL) was added to the hot solution (60 C) of the HL ligand (0.279 g, 1 mmol) in the same solvent (25 mL). The resulting mixture was stirred under reflux for 1 h whereupon the complexes precipitated. They were collected by filtration, washed with a 1:1 ethanol:water mixture and diethyl ether. The analytical data for C, H, N and S were repeated twice.

Biological Study

Fungicidal activity of the synthesized complexes in term of their inhibition to the linear growth of Fusarium solani, Rhizoctoni solani and Sclerotium rolfesii soil borne fungi.

Potato–dextrose agar (PDA) was used to evaluate the effect of the selected compounds under investigation on the mycelia linear growth of three tested fungi. Fifty milliliters of the aforementioned medium were poured into 150 mL conical flasks and autoclaved at 121 C for 20 min. Three drops of 25% lactic acid were added to prevent bacterial contamination. Dilutions for each of the tested compound wre carried out (v/v) by dissolving appropriate amounts of each compound in 10 mL DMSO. Equal volumes of DMSO containing diluted compounds were added to sterile molten (40 C) PDA to get a series of concentrations of 125, 250, 500 and 1000 ppm for each compound in PDA[13].

A zero (0) concentration treatment was prepared for each fungus, which contains equivalent volume of solvent only, and used as control. Compounds–amended PDA were dispensed aseptically into 9 cm diameter petridishes. Plugs of mycelium (4 mm diameter) were cut from the margins of actively growing cultures of the F. solani, R solani and S.rolfesii fungi and placed in the center of compound amended and unamended PDA plates with 4 replicate plates for each fungus. All plates were incubated at 25 ± 1 C. Colony diameter (in mm) was measured after 3 days for R.solani, S. rolfsii and 7–12 days for F. solani fungi and the percentage of growth inhibition was calculated for each compound. The estimated effective concentration (EC_{50}) which gives 50% inhibition of fungi radial growth, toxicity index (T.I.) and slopes of toxicity lines for each compound under investigation were determined and tabulated in Table 5.1.

Results and Discussion

Composition and Structures of the Complexes

The isolated solid complexes of Cr(III), Mn(II), Co(II), Ni(II), Cu(II) and Zn(II) ions with the HL ligand were subjected to elemental analyses (C, H, S and metal content), IR, magnetic studies, molar conductance and thermal analyses (TGA and DTA) to identify their tentative formulae in a trial to elucidate their molecular structures. The results of elemental analyses (Table 5.1), are in good agreement with those required by the proposed formulae. The formation of these complexes may proceed according to the following equations given below:

$$MCl_x + HL + H_2O + yH_2O \rightarrow [MCl_x(HL)(H_2O)yH_2O \quad (1)$$

M = Cr(III), Mn(II), Co(II), Ni(II), Cu(II), Zn(II); x = 2–3; y=0–4

$$CuSO_4 + HL \rightarrow [CuSO_4(HL)] \quad (2)$$

Molar Conductivity Measurements

The chelates were dissolved in DMF and the molar conductivities of 10^{-3} M of their solutions at 25 ± 2°C were measured. Table 5.1 shows the molar conductance values of the complexes. It is concluded from the results that the chelates are found to have molar conductance values of 8.68–23.45 Ω^{-1} mol^{-1} cm^2 indicating that these chelates are non–electrolytes. It, also, indicates the bonding of the sulphate or chloride anions to the metal ions.

Magnetic Susceptibility and Electronic Spectra Measurements

For the hexacoordinated Cr(III) complex, there are three spin–allowed transition in the electronic spectrum, ν_1: $^4B_{1g} \rightarrow {}^4E_g$ ($^4T_{2g}$), $^4B_{1g} \rightarrow {}^4B_{2g}$ ($^4T_{2g}$) and ν_3 $^4B_{1g} \rightarrow {}^4E_g$ ($^4T_{1g}$)[14,15]. The diffuse reflectance spectrum of the Cr(III) chelate shows three absorption bands at 18750 (ν_1), 26890 (ν_2) and 36450 (ν_3). The magnetic moment at room temperature is 3.86 B.M. which corresponds to three unpaired electrons for a d^3 Cr(III) ion and confirm octahedral geometry for this complex[14,15]. The diffuse reflectance spectrum of the Mn(II) complex shows three bands at 17570, 22442 and 26970 cm^{-1} assignable to $^4T_{1g} \rightarrow {}^6A_{1g}$, $^4T_{2g}(G) \rightarrow {}^6A_{1g}$ and $^4T_{1g}(D) \rightarrow {}^6A_{1g}$ transitions, respectively[14]. The magnetic moment value is 5.44B.M. which indicates the presence of Mn(II) complex in octahedral structure. The electronic spectrum of the Co(II) complex gives three bands at 15765, 18978 and 23430 cm^{-1} wave number regions. The bands observed are assigned to the transitions octahedral geometry around Co(II) ion[14,16,17]. The

magnetic susceptibility measurements lie at 4.95 B.M. (normal range for octahedral Co(II) complexes is 4.3–5.2 B.M.) is an indicative of octahedral geometry[14]. The region at 25990 cm^{-1} refer to the ligand to metal charge transfer band.

The Ni(II) complex reported herein has a room temperature magnetic moment value of 3.17 B.M.; which is in the normal range observed for octahedral Ni(II) complexes (μ_{eff} = 2.9–3.3 B.M.)[14,18]. This indicates that, the complex of .Ni(II) is six coordinate and probably octahedral[14,18]. The electronic spectrum in addition to show the $\pi-\pi^*$ and $n-\pi^*$ bands of free ligands, displays three bands in the solid reflectance spectrum at ν_1: 16350 cm^{-1}; $^3A_{2g}\rightarrow{}^3T_{2g}$ ν_2; 18922 cm^{-1} $^3A_{2g}\rightarrow{}^3T_{2g}$ (F) ν_3; 22754 cm^{-1}; $^3A_{2g}\rightarrow{}^3T_{1g}$ (P). The spectrum shows also a band at 25655 cm^{-1} which may attribute to ligand to metal charge transfer.

The reflectance spectra of Cu(II) chelates consist of a broad band centered at 17637 and 19467–20722 cm^{-1}. The ^2E_g and $^2T_{2g}$ states of the octahedral Cu(II) ion (d^9) split under the influence of the tetragonal distortion and the distortion can be such as to cause the three transitions $^2B_{1g}\rightarrow{}^2B_{2g}$; $^2B_{1g}\rightarrow{}^2E_g$ and $^2B_{1g}\rightarrow{}^2A_{1g}$ to remain unresolved in the spectra[19].

It was concluded that all three transitions lie within the single broad envelope centered at the same range previously mentioned. The magnetic moment of 1.98–2.02 B.M. falls within the range normally observed for octahedral Cu(II) complexes[14,19]. A moderate intense peak observed at 25364 cm^{-1} is due to ligand– metal charge transfer transition[14,19]. The complex of Zn(II) is diamagnetic. According to the empirical formula, an octahedral is proposed for this complex.

Table 5.1
Analytical and physical data of HL and its complexes

S. No.	Compound	Colour (% yield)	M.p. (°C)	% Found (Calcd.)					(μ_{eff}(B.M)	(m)[a]
				C	H	N	S	M		
1.	$(C_{12}H_{15}N_3S_2)$(HL)			54.20 (54.33)	5.60 (5.66)	15.72 (15.84)	24.0 (24.15)	–	–	–
2.	$(C_{12}H_{19}N_3MnO_2S_2Cl_2)$ $[MnCl_2(HL)(H_2O)]H_2O$	Yellow (73)	>300	32.70 (32.79)	4.30 (4.45)	9.72 (9.83)	14.85 (14.79)	12.75 (12.86)	5.44	12.35
3.	$(C_{12}H_{19}Cl_3CrN_3O_2S_2)$ $[CrCl_3(HL)]2H_2O$	Green (82)	>300	31.25 (31.23)	4.0 (4.13)	9.0 (9.14)	13.80 (13.92)	11.20 (11.31)	3.86	8.68
4.	$(C_{12}H_{19}Cl_3CoN_3O_2S_2)$ $[CoCl_2(HL)(H_2O)]H_2O$	Green (70)	>300	33.30 (33.41)	4.20 (4.40)	9.65 (9.74)	14.73 (14.85)	13.50 (13.67)	4.92	13.67
5.	$(C_{12}H_{19}Cl_3NiN_3O_2S_2)$ $[NiCl_2(HL)(H_2O)]H_2O$	Brown (68)	>300	33.35 (33.43)	4.31 (4.41)	9.65 (9.75)	14.76 (14.85)	13.55 (13.63)	3.17	23.45
6.	$(C_{12}H_{25}Cl_2CuN_3O_2S_2)$ $[CuCl_2(HL)(H_2O)]4H_2O$	Brown (80)	>300	29.31 (29.41)	5.0 (5.10)	8.48 (8.57)	13.0 (13.07)	12.85 (12.97)	2.02	21.98
7.	$(C_{12}H_{15}CuN_3O_4S_3)$ $[CuSO_4(HL)]$	Green (65)	>300	33.82 (33.91)	3.42 (3.53)	9.80 (9.89)	22.50 (22.61)	14.86 (14.96)	1.98	12.9
8.	$(C_{12}H_{23}Cl_2ZnN_3O_4S_3)$ $[ZnCl_2(HL)(H_2O)]3H_2O$	Brown (75)	>300	30.30 (30.42)	4.73 (4.85)	8.80 (8.87)	13.40 (13.52)	13.72 (13.80)	Diam.	17.8

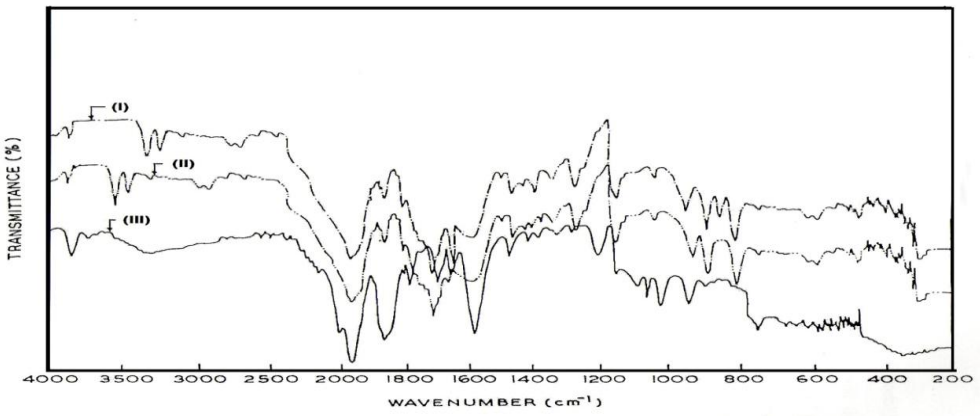

Fig (5.1) IR - Spectra of the complexes
(i) $(C_{12}H_{15}N_3S_2)$ (ii) $[Mn(C_{12}H_{15}N_3S_2)Cl_2.H_2O](H_2O)$ (iii) $[Cr(C_{12}H_{15}N_3S_2)Cl_2.]2H_2O$

IR Spectra and Mode of Bonding

The infrared spectra of the title ligand and its metal(II) or metal(III) complexes and important characteristic absorption bands, along with their proposed assignments, are summarized in Table 5.2. The IR spectra of the complexes are very similar to each other, except some slight shifts and intensity change of a few vibration bands caused by different metal ions, which indicate that the complexes have similar structures. However, there are some significant changes between the metal complexes and their free ligand for chelation as expected. The coordination mode and sites of the ligand to the metal ions were investigated by comparing the infrared spectra of the free ligand with its metal complexes. Upon coordination, it is noteworthy that the peak at 1678 cm^{-1} attributed to ν(C=N) vibration originating from N–3 imidazole ring, is disappeared or shifted by 24–30 cm^{-1} on complexation, indicating coordination of N–3 atom to metal ions[20]. In addition, IR spectrum of the ligand revealed a sharp band at 1270cm^{-1} due to ν(C=S) of side chain, which is slightly shifted to higher frequency at about 3–7 cm^{-1} after complexation in all complexes, suggesting that sulfur atom of the side chain also contributes to the complexation. The band observed at 1088 cm^{-1} in the free HL ligand is appeared at relatively lower field (1059–1070 cm^{-1}) in the complexes which may indicates coordination via the C–S group[21].

The IR bands at 840 and 750 cm^{-1}, ν(H_2O) of coordinated water, is in indication of the binding of the water molecules to the metal ions. New bands are found in the spectra of the complexes in the regions 552–622, 480–560 and 428–439 cm^{-1}, which are assigned to ν(M–N), ν(M–S) and ν(M–S) stretching vibrations[21,22]. Therefore, from the IR spectra, it is concluded that HL ligand behaves as a neutral dentate ligand coordinated to the metal ions via the imidazole N–3, C=S and C–S groups.

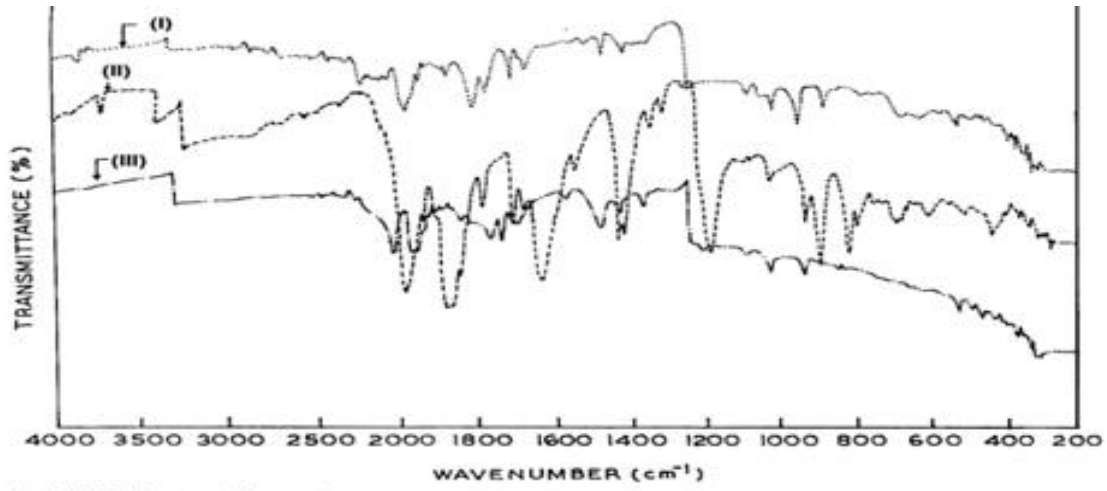

Fig (5.2) IR - Spectra of the complexes
(i) $[Co(C_{12}H_{15}N_3S_2)Cl_2.H_2O](H_2O)$ (ii) $[Ni(C_{12}H_{15}N_3S_2)Cl_2.H_2O](H_2O)$ (iii) $[Cu(C_{12}H_{15}N_3S_2)Cl_2(H_2O)]4H_2O$

Thermal Analyses (TGA, DrGA and DTA)

In the present investigation, heating rates were suitably controlled at 10 C min^{-1} under nitrogen atmosphere and the weight loss was measured from the ambient temperature up to ≅1000°C. The data are listed in Table 5.3. The weight losses for each chelate are calculated within the corresponding temperature ranges. The different thermodynamic parameters are listed in Table 5.4. The thermogram of $[MnCl_2(HL)(H_2O)]H_2O$ chelate shows four decomposition steps within the temperature range 30–850°C. The first step of decomposition within the temperature range 30–90°C corresponds to the loss of water molecule of hydration with a mass loss of 4.62% (calcd. 4.09%). The energy of activation is 33.23 kJ mol^{-1}. The subsequent steps (90–850 C) correspond to the removal of the organic part of the ligand and 2HCl molecules (mass loss = 80.47%; calcd = 80.0%) leaving MnO as a residue. The overall weight loss amounts to 85.09% (Calcd. 84.09%).

Table 5.2
IR data (4000–400 cm^{-1}) of HL and its metal complexes

Compound	ν(C=N)	ν(C=S)	ν(C–S)	ν(M–N)	ν(M–S)	ν(M–S)
$(C_{12}H_{15}N_3S_2)$ (HL)	1678 m	1270sh	1088sh	–	–	–
$(C_{12}H_{19}N_3MnO_2S_2Cl_2)$	Disappear	1274sh	1066w	570w	470w	439w
$(C_{12}H_{19}Cl_3CrN_3O_2S_2)$	Disappear	1273s	1067m	615m	560w	428m
$(C_{12}H_{19}Cl_2CoN_3O_2S_2)$	Disappear	1275sh	1069m	557w	483m	428w
$(C_{12}H_{19}Cl_2NiN_3O_2S_2)$	Disappear	1274sh	1070m	622w	520w	430w

($C_{12}H_{25}Cl_2CuN_3O_5S_2$)	1706sh	1277m	1068sh	621m	540w	434m
($C_{12}H_{15}CuN_3O_4S_3$)	1656m	1275sh	1070m	616m	485m	436m

($C_{12}H_{23}Cl_2ZnN_3O_4S_2$)	Disappear	1277sh	1059sh	552m	485m	433m

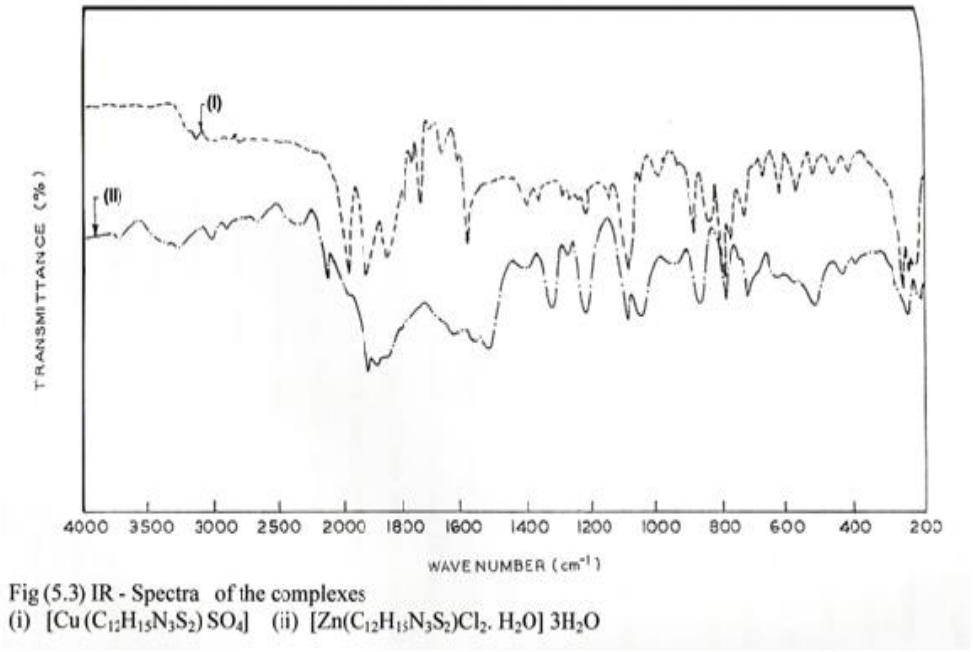

Fig (5.3) IR - Spectra of the complexes
(i) $[Cu(C_{12}H_{15}N_3S_2)SO_4]$ (ii) $[Zn(C_{12}H_{15}N_3S_2)Cl_2.H_2O]3H_2O$

The TGA curve of the Cr(III) chelate shows four stages of decomposition within the temperature range of 30–800 C. The first stage within the temperature range from 30 to 145°C corresponds to the loss of two water molecules of hydration (mass loss = 7.85; calcd = 7.60). The energy of activation for this dehydration step is 55.25 kJ mol^{-1}. While the subsequent (2^{nd}, 3^{rd} and 4^{th}) stages involve the loss of 3HCl and ligand molecules with a mass loss of 77.97% (calcd. 77.61%). The overall weight loss amounts to 85.82% (calcd. 85.21%).

On the other hand, $[CoCl_2(HL)H_2O)].H_2O$ chelate exhibits four decomposition steps. The first step in the temperature range 30–85°C (mass loss = 4.81%; calcd. For H_2O; 4.05%) may accounted for the loss of water molecule of hydration. The energy of activation for this step is 46.89 kJ mol^{-1}. As shows in Table 5.4 the mass losses of the remaining decomposition steps amount to 79.92% (calcd. 79.10%). They correspond to the removal of 2HCl and HL molecules leaving CoO as a residue. The values of energy activation for these steps are 105.4, 184.3 and 256.7 kJ mol^{-1} for the 2^{nd}, 3^{rd} and 4^{th} steps,
respectively.

$[NiCl_2(HL)H_2O)].H_2O$ complex is thermally decomposed in four decomposition steps within the temperature range of 30–850°C. The first decomposition step with an estimated mass loss of 8.63% (calcd. Mass loss – 8.09%) within the temperature range 30–160°C may be attributed to the loss of hydrated and coordinated water molecules. The activation energy is 50.59 $kJmol^{-1}$. The remaining decomposition steps (three steps) found within the temperature range 160–850°C with an estimated mass loss of 71.07% (calcd. Mass loss = 71.46%) which are reasonably accounted for the removal of 2HCl and HL ligand as gases leaving NiS as a residue. The values of the activation energy are 118.7, 192.6 and 263.4 kJ mol^{-1} for the 2^{nd}, 3^{rd} and 4^{th}steps,respectively.

Table 5.3: Thermoanalytical results (TGA and DTA) of HL and its metal complexes

Complex	TG range (°C)	DTA (°C)	n*	Mass loss	Total mass loss / Estimated (calcd) %	Assignment	Metallic residue
(1)	30–90 90–850	55(+), 140(+) 170(–), 230(–), 360(–), 450(–), 550(–), 660(–)	1 3	4.62 (4.09) 80.47 (80.00)	85.09 (84.09)	Loss of H_2O Loss of 2HCl and HL	MnO
(2)	30–145 145–800	40(–), 72(+), 190(+), 210(–), 230(+), 430(–), 520(–), 650(+), 710(–)	1 3	7.85 (7.60) 77.97 (77.61)	85.82 (85.21)	Loss of $2H_2O$ Loss of 3HCl and HL	CrS
(3)	30–85 85–800	50(+), 120(+), 205(+), 230(–), 250(+), 275(+), 494(+), 620(–)	1 3	4.81 (4.05) 79.92 (79.10)	84.73 (83.15)	Loss of H_2O Loss of 2HCl and HL	CuO
(4)	30–160 16–850	60(+), 95(–), 160(+), 195(–), 250(–) 320(–), 450(+), 530(–), 680(–)	1 3	8.63 (8.09) 71.07 (71.46)	79.70 (79.55)	Loss of $2H_2O$ Loss of 2HCl and HL	NiS
(5)	30–150 150–800	50(–), 80(+), 110(+), 150(–), 210(–), 250(+), 320(–), 440(–) 550(–)	1 2	14.91 (14.30) 69.51 (69.91)	84.42 (84.21)	Loss of $4H_2O$ Loss of 2HCl and HL	CuO

n*=number of decomposition steps. (1) $[MnCl_2(HL)(H_2O)]H_2O$, (2) $[CrCl_3(HL)]2H_2O$, (3) $[CoCl_2(HL)(H_2O)]H_2O$, (4) $[NiCl_2(HL)(H_2O)]H_2O$, (5) $[CuCl_2(HL)(H_2O)]4H_2O$; HL–($C_{12}H_{15}N_3S_2$); (+)– endothermic and (–) = exothermic

Table 5.4

Thermodynamic data of the thermal decomposition of metal complexes of HL

Complex	Decomp. Temp. (°C)	E* (kJ mol^{-1})	A(S^{-1})	ΔS^+(kJ mol^{-1})	ΔH^+(kJ mol^{-1})	ΔG^+(kJ mol^{-1})
$[MnCl_2(HL)(H_2O)].H_2O$	30–90 90–170 170–450 450–850	33.23 74.67 109.1 145.3	3.20×10^7 5.55×10^{10} 7.11×10^{11} 6.21×10^6	–48.72 –100.7 –164.6 –220.5	53.52 81.69 108.6 162.8	70.4 126.5 188.7 223.6
$[CrCl_3(HL)].2H_2O$	30–145 145–300 300–650 650–800	55.25 63.99 145.6 198.7	3.66×10^7 7.63×10^9 2.99×10^{13} 4.68×10^{11}	–66.95 –128.7 –203 –256.4	94.82 151.5 225.9 302.5	79.81 137.4 235.6 335.6
$[CoCl_2(HL)(H_2O)].H_2O$	30–85 85–250 250–510 510–800	46.89 105.4 184.3 256.7	4.66×10^{10} 1.98×10^7 5.19×10^{13} 6.35×10^8	–39.83 –129.8 –194.6 –275.3	50.63 90.36 162.7 256.3	72.63 135.7 244.6 303.4
$[NiCl_2(HL)(H_2O)].H_2O$	30–160 160–470 470–620 620–800	50.59 118.7 192.6 263.4	2.69×10^7 5.47×10^{10} 6.07×10^{11} 4.69×10^7	–40.69 –75.44 –103.2 –172.6	66.77 136.3 217.6 249.6	86.88 186 245 277.8
$[CuCl_2(HL)(H_2O)].4H_2O$	30–150 150–400 400–800	33.67 96.85 188.2	5.62×10^{10} 2.98×10^{14} 3.89×10^{12}	–30.83 –99.87 –204.5	55.63 130.4 262.7	78.63 145.7 274.6

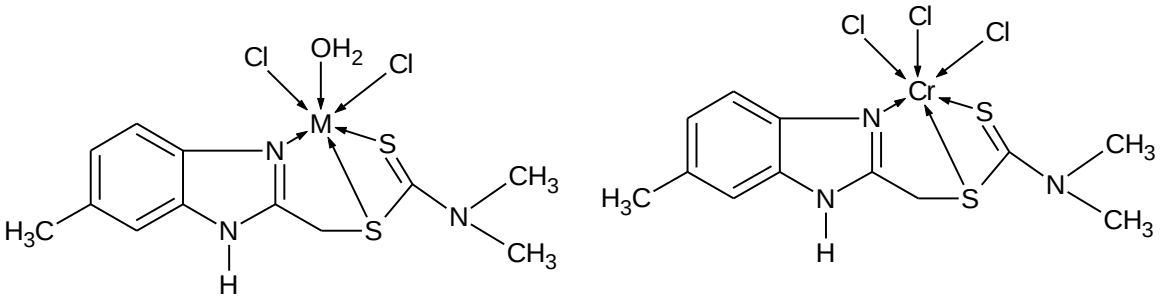

M = Mn(II), Co(II), Ni(II), Cu(II) and Zn(II)

Fig. 2. Suggested structure of metal complexes

The TGA curve of the $[CuCl_2(HL)(H_2O)].4H_2O$ chelate represents three decomposition steps as shown in Table 5.3. The first step of decomposition within the temperature range 30–150°C corresponds to the loss of four hydrated water molecules with a mass loss of 14.91% (Calcd. for $4H_2O$; 14.30%). The energy of activation for this dehydration step is 33.67 kJ mol^{-1}. The remaining steps of decomposition within the temperature range 150–800°C correspond to the removal of HL ligand as gases with an energy of activation for these steps of 96.85 and 188.2 kJ mol^{-1} for the 2nd and 3rd steps, respectively. The overall weight losses amount to 84.82% (calcd. 84.21%). The data given also in Table 5.3 show the DTA results obtained during the thermal decomposition of the complexes. All the complexes give an endo– and exo–thermic peaks within the temperature ranges of decomposition.

Kinetic data

The thermodynamic activation parameters of decomposition processes of dehydrated complexes namely activation energy (E*), enthalpy (ΔH*), entropy (ΔS*) and Gibbs free energy change of the decomposition (ΔG*) were evaluated graphically by employing the Coats–Redfern relation[23]. The entropy of activation (ΔS*), enthalpy of activation (ΔH*) and the free energy change of activation (ΔG*) were calculated.

The data are summarized in Table 5.4. The activation energies of decomposition are found to be in the range 22.95–243.4 kJ mol^{-1}. The high values of the activation energies reflect the thermal stability of the complexes. The entropy of activation is found to have negative values in all the complexes which indicates that the decomposition reactions proceed with a lower rate than the normal ones.

Structural interpretation

The structures of the complexes of HL with Cr(III), Mn(II), Co(II), Ni(II), Cu(II) (Cl^- and SO_4^{2-}) and Zn(II) ions are confirmed by the elemental analyses, IR, molar conductance, magnetic, solid reflectance, mass and thermal analysis data. Therefore, from the IR spectra, it is concluded that HL behaves as a neutral tridentate ligand coordinated to the metal ions via the imidazole N–3 and two side chain S atoms. From the molar conductance data, it is found that the complexes are non–electrolytes. On the basis of the above observations and from the magnetic and solid reflectance measurements, octahedral geometries are suggested for the investigated complexes except $CuSO_4$ complex has square planar geometry. As a general conclusion, the investigated metal complex structures can be given as shown in Fig. 2.

Fungicidal activity

Data in Table 5.5 shows that the EC_{50} values of the prepared complexes of R. solani and S. rolfesii fungi are lower than that of the corresponding free ligand. This means that, the complexation process increases the fungicidal potency on these two tested fungi. The ranges of EC_{50} values of the complexes of R solani fungus are 205.46–305.14 and 196.64–393.58 ppm on S. rolfsii but that of the free ligand are 521.00 and 800.12 ppm on R. solani and S. rolfesii, respectively. The high fungitoxic effect of the complexes than the free ligand can be understood in term of chelation theory which stated that, upon complexation the polarity of the metal ion gets reduced which increases the lipophilicity of the metal complexes, facilitating them to cross the cell membrane easily[24].

In contrast F. solani fungus shows higher resistance to the synthesized complexes than the free ligand with exception of the cobalt and nickel complexes. Generally, cobalt complex shows the highest fungicidal activity as it has the lowest EC_{50} values on the three tested fungi. These values are 353.55, 205.45 and 196.84 ppm for F.solani, R. slain and S.rolfesii fungi, respectively. Consequently, we formulated this complex to make it commercially available as a local fungicide after satisfying all required studies.

Formulation

The main technique is used to apply the active ingredients of pesticides in the field. Beside the ability of formulation to spread the small amount of active ingredient over a large area, it also improves its pesticidal activity in the field.

Table 5.5
Fungicidal activity of the new synthesized complexes on the three soil borne fungi

Complex	F. solani			R. solani			S. rolfesii		
	EC_{50} (ppm)	Slope	T.I.a	EC50 (ppm)	Slope	T.I.a	EC50 (ppm)	Slope	T.I.a
$[CuSO_4(HL)]$	2344.1	0.67	15.1	232.5	1.63	88.4	261	0.85	75.3
$[CuCl_2(HL)(H_2O)].4H_2O$	662.8	3.2	53.3	253.4	2.62	81.1	282.1	1.58	69.7
$[CoCl_2(HL)(H_2O)].H_2O$	353.5	2.2	100	205.5	1.81	100	196.6	1.97	100
$[CrCl_3(HL)].2H_2O$	525.6	2.36	67.3	220.7	1.68	93.1	389	1.72	50.5
$[MnCl_2(HL)(H_2O)].H_2O$	535.8	0.77	66	282.3	2.62	72.8	294.3	2.07	66.8
$[NiCl_2(HL)(H_2O)].H_2O$	469.1	2.14	75.4	227.2	1.34	90.4	227.6	1.89	86.4
$[ZnCl_2(HL)(H_2O)].3H_2O$	555.2	2.05	63.7	305.1	3.26	67.3	393.6	2.61	50
$HL(C_{12}H_{15}N_3S_2)$	526.1	0.38	67.2	5.21	0.62	39.4	800.1	3.32	24.6

[a]Toxicity index is the % of activity of the tested compounds to the most potent one whose T.I. in 100.
HL– $(C_{12}H_{15}N_3S_2)$

Table 5.6
Fungicidal activity of the local formulation (25% WP) and the standard fungicide (Monceren 25% WP) on the three tested fungi

Conc. (ppm)	F. solani		R. solani		S. rolfesii	
	Mean growth zone (mm)	% of inhibition	Mean growth zone (mm)	% of inhibition	Mean growth zone (mm)	% of inhibition
500	24.5	72.8	27.4	69.5	0	100
400	27	70	40.7	54.8	11.3	87.4
300	30	66.7	43	52.2	24	73.3
200	32.7	63.7	47	47.8	32.2	64.1
100	45	50	57	36.6	90	0
Control(0)	90.9	0	90.9	0	90.0	0
EC_{50}*	90.94 ppm		207.52 ppm		206.23 ppm	
EC_{50}**	2467.70 ppm		48.0 ppm		2309.18 ppm	

EC_{50}* is the effective concentration of the new formulation.
EC_{50}** is the effective concentration of the standard fungicide (Monceren 25% WP

Depending on the physico–chemical properties of the active ingredient as well as the type of pest, we should select the type of formulation. In this work we formulated the cobalt complex in the form of 25% wettable powder (25% WP). The local formulation passed successfully the required tests according to the standard method[(25)]. The components of the formulation are listed as follows

The active ingredient (co–complex)	25.00%	w/w
Anionic surfactant	20.00%	w/w
Dispersing agent	4.00%	w/w
Antifoaming agent	1.00%	w/w
Carrier	50.00%	w/w
Total	100%	w/w

To determine the fungicidal potency of the new formulation we evaluated its activity against the same fungi and compared it with the commercially used fungicide (Monceren 25% WP) by using different ranges of dilutions.

From data in Table 5.6 it is evident that the inhibition activity of the formulation, to the fungi mycelia growth, increases as the concentration increases. The EC_{50} values of the new formulation are 90.94, 207.52, 208.23 ppm but that of the standard fungicide are 2467.70, 48.50, 2309.18 ppm on F. solani, R. solani and S. rolfesii fungi. Respectively. Data shown reflects the higher fungicidal activity of the new formulation as compared with the standard fungicide on F. solani and S. rolfesii fungi but not for R. solani fungus.

Conclusion

1. Many transition metal complexes were synthesized from the benzimidazole dithiocarbamate ligand (HL).
2. Complexation process increases the fungicidal activity of the ligand.
3. Cobalt complex was found to be the most potent one against the three tested soil borne fungi so it was formulated as 25% WP.
4. Fungicidal activity of the new formulation was evaluated and compared with the standard fungicide (Monceren 25% WP).
5. Data obtained showed the higher fungicidal activity of the new formulation than the standard fungicide in most cases.

References

1. Walba, H. & Isensee, R. W. Acidity constants of some arylimidazoles and their cations. J. Org. Chem. 26, 2789-2791 (1961).
2. H. A. Barker, R. D. Smyth, H. Weissbach, J. I. Toohey, J. N. Ladd, and B. E. Volcani (February 1, 1960). "Isolation and Properties of Crystalline Cobamide Coenzymes Containing Benzimidazole or 5,6-Dimethylbenzimidazole". Journal of Biological Chemistry 235 (2): 480–488. PMID 13796809.
3. R. Jackstell, A. Frisch, M. Beller, D. Rottger, M. Malaun and B. Bildstein (2002). "Efficient telomerization of 1,3-butadiene with alcohols in the presence of in situ generated palladium(0)carbene complexes". Journal of Molecular Catalysis A: Chemical 185 (1–2): 105–112.doi:10.1016/S1381-1169(02)00068-7.
4. H. V. Huynh, J. H. H. Ho, T. C. Neo and L. L. Koh (2005). "Solvent-controlled selective synthesis of a trans-configured benzimidazoline-2-ylidene palladium(II) complex and investigations of its Heck-type catalytic activity". Journal of Organometallic Chemistry 690 (16): 3854–3860. doi:10.1016/j.jorganchem.2005.04.053
5. B.V. Kumar, V.M.Reddy, Indian J. Chem. Sect. 8, 248 (1985) 1298.
6. J.F.Olin, (U.S. 3 (1975) 860], C.A., 82 (1975) 155907.
7. L.Mishra, S.Kagini, J. Indian Chem. Soc. 76 (1999) 500.
8. E.R.Gulgun, N.Altanlar, A.Akin, Ilfarmaco, 51 (1996) 413; C.A., 125 (1996) 221699.
9. M.Tuncbilek, H.Goker, R.Ertan, R.Eryigit, E.Kendi, N.Altanlar, Arch. Pharm. (Weinheim, Ger), 330 (1997) 372.
10. Y.Maki, H.Kimoto, S.Fujii, H.Muramatsu, N.Hirata, K.Kamoshita, T.Yano, M.Hirano, [Jpn. Kokai Tokkyo Koho JP 01, 135 (1989) 773 (89, 135, 773)]; C.A. 112 (1990) 7485.
11. W.Lunkenteimer, B.Baasner, F.Lieb, C.Erdelen, J. Hartwig, U.Wachendroff, Newmann, W.Stendel, V.Goergens, [Ger. Offen, DE 4, 237 (1994) 548]; C.A., 122 (1995) 160636.
12. J.L.Miessel, [U.S. 4,000 (1976) 295], C.A., 86 (1977) 140050.
13. X.Hansheng, F.Zice, L.Xiufang, S.Yaojun, Z.Baixin, Wuhan Dauxe Xuebao, Ziran Kexueban; 71 (1990), C.A., 114 (1991) 62369.
14. S.E.Lazer, R.M.Matteo,J.G.Possanza, J. Med. Chem. 30 (1987) 726.
15. Z.Ejmocki, Z.Ochal, [Pol. PL 139m (1987) 912]; C.A., 109 (1988) 73428.
16. H.M.F.Madkour, A.A.Farag, S.Sh. Ramses, N.A., Ibrahim, Phosphorus, Sulfur Silicon 181 (2006) 255.
17. D.M.Tremblay, B.G.Talbot, O.Garisse, Plant, Dis. 87 (2003) 570.
18. F.A.Cotton, G.Wilkinson, C.A.Murillo, M.Bochmann, Advanced Inorganic Chemistry, Sixth ed., Wiley, New York, 1999.
19. M.K.Koley, S.C.Sivasubramanian, B.Varghese, P.T.Manoharan, A.P.Koley, Inorg. Chim. Acta 361 (2008) 1485.
20. G.G.Mohamed, Z.H.Abd, El. Wahwb, J. Thermal Anal. 73 (2003) 347.
21. M.M.Omar, G.G.Mohamed, Spectrochim. Acta (Part A), 61 (2005) 929.
22. G.G.Mohamed, N.E.A., El–Gamel, F.A.Nour El–Dien, Synth. React. Inorg. Met.–Org. Chem. 31 (2001) 347.
23. J.Kohout, M.Hvastijova, J.Kozisek, J.G.Diaz, M.Valko, L.Jager, I.Svoboda, Inorg. Chim. Acta 287 (1999) 186.
24. G.G.Mohammed, N.E.A.El–Gamel, F.Teixidor,Polyhedron 20 (2001) 2689.
25. A.A.Soliman, G.G.Mohamed, Thermochim. Acta 421 (2004) 151.
26. M.A.Zayed, F.A., Nour El–Dien, G.G.Mohamed, N.E.A. El–Gamel, J. Mol. Struct. 841 (2007) 41.
27. A.W.Coats, J.P.Redfern, Nature 20 (1964) 68.
28. C.M.Thimmaiah, G.T.Chadrappa, W.D.Lloyd, Inorg. Chim. Acta 107 (1985) 281.
29. FAO and WHO joint meeting on pesticides specifications (JMPS), [Manual on Development and Use of FAO and WHO Specifications for Pesticides], Rome, 2006.